SUPPORTING INFORMATION FOR

A DNA origami fiducial for accurate 3D AFM imaging

Pauline J. Kolbeck[1,2,3], Mihir Dass[1,2], Irina V. Martynenko[1,2,*], Relinde J.A. van Dijk-Moes[3], Kelly J.H. Brouwer[3], Alfons van Blaaderen[3], Willem Vanderlinden[1,2,3], Tim Liedl[1,2], Jan Lipfert[1,2,3,*]

[1,2]Department of Physics and Center for NanoScience, LMU Munich, Amalienstrasse 54, 80799 Munich, Germany
[3]Department of Physics and Debye Institute for Nanomaterials Science, Utrecht University, Princetonplein 1, 3584 CC Utrecht, The Netherlands

[*]Correspondence: Irina.Martynenko@physik.uni-muenchen.de; J.Lipfert@uu.nl

Supplementary Materials and Methods
Supplementary Table S1
Supplementary Figures S1-S7

Supplementary Materials and Methods

DNA origami design and assembly

The DNA origami AFM fiducial structure was designed using caDNAno[1] (design schematics in Figure S1). The staircase-like structure consists of eight layers of parallel helices packed on a square lattice. The designed length of the structure is 200 base pairs, the width is ten helices. The number of DNA helices in the layers is varied to obtain four discrete steps with equal x-y areas and heights of one, two, five, and eight helices. Sequences and the caDNAno design of the DNA origami AFM fiducial structure can be found as AFMRuler.xls and AFMRuler.json as a part of the zip archive AFMRuler.zip in the Supporting Information. The *x*-*y* dimension of each step in our design is approximately 17 nm × 20 nm (50 bp×10 helices), which provides a sufficient number (>20 points per height plateau) of independent measurement points for calibration[2] and ensures mechanical stability during the AFM measurement. We used the square lattice geometry and corrected the design for internal twist[3, 4] to obtain a flat surface of the 'stairs'.

Design-specific staple strands were purchased from IDT Technologies, the scaffold strand p8634 was produced from M13 phage replication in *E. coli*. Scaffold strand and staple strands were mixed at 1:5 scaffold:staple ratio with target concentrations of 30 nM and 150 nM (each staple), respectively in 10 mM Tris Base, 1 mM EDTA buffer with 18 mM magnesium chloride (TE/Mg^{2+}). 50 µL volumes of staple/scaffold mixture were heated up to 65°C for 5 min and annealed from 65°C to 20°C at -0.2°C/min in a PCR machine. The DNA origami structures were purified from excess staples using 100 kD molecular weight cut-off filters (Amicon Ultra-0.5 Centrifugal Filter Units with Ultracel-100 membranes). The 24-helix-bundle (24HB) structure[5] was folded in a similar fashion using the p8064 scaffold strand and purified using the PEG precipitation method adapted from Wagenbauer *et al.*[6].

TEM sample preparation and imaging

5 µL of sample solution was incubated for 30 s – 5 min, depending on concentration, on glow discharged TEM grids (formvar/carbon, 300 mesh Cu; Ted Pella) at room temperature. After incubation on the grids, the sample was wicked off by bringing the grid into contact with a filter paper strip. Samples containing DNA origami went through an additional staining step with a 2% uranyl formate aqueous solution containing 25 mM sodium hydroxide. After incubating and wicking the sample off, a 5 µL drop of staining solution (2% uranyl formate aqueous solution containing 25 mM sodium hydroxide) was applied to the grid, immediately wicked off, followed by applying another 5 µL drop of staining solution. This drop was allowed to incubate on the grid for 10 seconds and then wicked off. The grid was allowed to dry for 5 minutes before imaging. Imaging was performed with a JEM1011 transmission electron microscope (JEOL) operated at 80 kV.

Synthesis of SiO_2 nanoparticles

Silica particles were synthesized with a one-step synthesis based on previous literature[7, 8]. All glassware was etched of residual silica via a base bath (2−3 days in a saturated solution of KOH in isopropanol, rinsed with milliQ water). The particles were synthesized as follows: in a 500 mL 1-neck flask, 181 mg (6 mM) L-arginine (98%, Sigma-Aldrich) were dissolved in 169 mL milliQ water. The mixture was heated to 30 °C and stirred slowly (200 rpm). After 1 h, 11.2 mL (49 mmol) TEOS (tetraethoxysilane; 98%, Sigma-Aldrich) was added slowly via the wall and a two layered system formed (top: TEOS, bottom: water). The reaction mixture was stirred for 1 week to complete the synthesis. The resulting particles were stored at room temperature in the dark and used without further processing.

AFM sample preparation

For the AFM samples, we deposited 20 µL of a buffered solution (10 mM Tris Base, 12.5 mM $MgCl_2$,1 mM EDTA, pH 8.35; AFM buffer) containing the fiducial structures (at different concentrations between 1 and 10 nM) either on freshly cleaved bare muscovite mica or on aminopropylsilatrane (APS)-coated mica or poly-L-lysine coated mica. The sample was incubated 5 minutes before washing with 20 mL milliQ water and drying with a gentle stream of filtered argon gas. The APS coating was performed following the protocol from Shlyakhtenko *et al.*[9]. The poly-L-lysine coated mica was prepared as described previously[10] by depositing 20 µL 0.01%-poly-L-lysine on freshly cleaved muscovite mica for 30 seconds and subsequently rinsing the surface with 30 mL of milliQ water before drying with a gentle stream of filtered argon gas.

For the liquid measurements, 2.5 mL of the buffered solution was added to the sample after incubation. For the co-deposited samples, we pre-mixed the fiducial structures with the corresponding sample (at varying concentrations between 1 and 10 nM) prior to deposition in AFM buffer. The samples were incubated, washed, and dried as described above.

For the DNA-protein complex sample, we first mixed linearized plasmid pU3U5 (4.751 kbp; Mini-HIV DNA, see Cherepanov *et al.*[11]) with HIV-I IN in sodium buffer (10 mM Tris-HCl, 90 mM NaCl; 5 mM $MgCl_2$) to a final concentration of 1 ng/ul DNA and 1 µM of protein. Next, we added the fiducial structures at a final concentration of 1 nM and deposited 20 µL of the mixture on APS-coated mica. The sample was incubated, washed, and dried as described above.

AFM imaging

The dry AFM images were recorded in tapping mode at room temperature using the Nanowizard Ultraspeed 2 (JPK, Berlin, Germany) with silicon tips (FASTSCAN-A, drive frequency 1400 kHz, tip radius 5 nm, Bruker, Billerica, Massachusetts, USA). Images were scanned over different fields of view and with various pixel sizes (indicated for each image) with a scanning speed of 5 Hz. The free amplitude varied from 20 to 30 nm. The amplitude setpoint was set to 80% of the free amplitude and adjusted to maintain good image resolution.

The liquid AFM images were recorded in peak-force tapping mode at room temperature, also using the Nanowizard Ultraspeed 2 (JPK, Berlin, Germany) with silicon tips (BL-AC40TS, drive frequency 25 kHz in water, tip radius 10 nm, Olympus, Tokyo, Japan). Images were scanned over different fields of view and with various pixel sizes (indicated for each image). The peak force was set to 200 pN. For some measurements we use an external polycrystalline tip characterization sample (PA01 AFM Tip Evaluation Sample, NanoAndMore GmbH, Wetzlar, Germany) with hard sharp pyramidal nanostructures with base length in the range 50 - 100 nm and height 50 - 150 nm, and radius of curvature of the sharpest edges below 5 nm.

AFM image analysis

For this work, postprocessing of AFM data was performed in the software SPIP (v.6.4, Image Metrology, Hørsholm, Denmark), which has implemented blind peak reconstruction as well as image deconvolution following Villarrubia's protocol[12]. We note that while we used SPIP for all image processing, other AFM post-processing softwares, such as Gwyddion, have also incorporated blind tip reconstruction routines with implementations very similar to SPIP. Here, we will give detailed instructions for tip characterization and image reconstruction for SPIP and Gwyddion. An example of a fiducial image recorded with a FASTSCAN-A cantilever can be found in Image_Reconstruction_Example_SPIP_Gwyddion.zip as Supporting Data, the resulting reconstructed images are also shown in Supplementary Figure S7.

AFM postprocessing with SPIP

First, the images were flattened (*Modify → Global leveling*) and line-wise leveled (*Modify → Linewise leveling*). Next, the tip was characterized via blind tip reconstruction. To this end, we either used the entire image or (in case of co-deposition or contamination of the sample) selected a subset of fiducial structures (*General → Area of interest*). Next, we used the tip characterization tool (*Analyze → Tip*) and specified the tip size in x and y as number of pixels (*Tip characterization → Size X and Y*). For FASTSCAN-A cantilevers, we took the manufacturer's specified tip radius of 12 nm as a starting point for the blind tip reconstruction (for example, for a FASTSCAN-A cantilever with a tip diameter of 24 nm and an image resolution of 1.6 nm/pixel, the tip size would correspond to 15 pixels). We typically used 5 iterations (more iterations did not to improve tip reconstruction in our experience, but could be an option for troubleshooting the procedure, e.g. for a particularly challenging sample). The resulting tip shape was saved (*Tip characterization → Save tip*) and then loaded (*Tip characterization → Load tip*) to correct (*Tip characterization → Deconvolute*) the same or another image scanned by the same tip. Here, too, the tip size had to be adjusted to the corresponding size in pixel so that the resolution is not lost (*Tip characterization → Size X and Y*). As a useful quality control, SPIP also calculates an uncertainty map. In this map, the areas of the image where the tip did not touch the surface in a single point, but in multiple points (so not with the tip apex but with the side), are highlighted in red, so that, for example, a larger area is shown in red when a blunt tip is used than when the same area was scanned with a sharp tip.

AFM postprocessing with Gwyddion

Gwyddion is an open source software for scanning probe microscopy data visualization and analysis (http://gwyddion.net/). Post-processing of AFM data in Gwyddion works very similarly to SPIP. Tip reconstruction in Gwyddion using the blind tip reconstruction algorithm is described in detail in the Gwyddion online user guide: http://gwyddion.net/documentation/user-guide-en/tip-convolution-artefacts.html.

In brief, the images first need to be flattened (*Data process → Level → Plane level*) and line-wise leveled (*Data process → Correct data → Align rows (Polynomial degree 2, Direction: horizontal)*). In the case of co-deposition, at least 10 fiducials are selected with one or several masks (*Tools → Edit mask (Mode: add selection to mask)*). As a prerequisite for blind tip reconstruction, the tip is first modeled (*Data Process → SPM modes → Tip → Model tip*) using the manufacturer's tip specifications (for example for a FASTCAN-A cantilever, Tip type: pyramid, Number of sides: 3, Tip slope: 15°, Tip rotation: 0°, Tip apex radius: 10 nm). Next, the tip is characterized using the blind tip estimation algorithm (*Data Process → SPM modes → Tip → Blind Estimation*). The blind tip estimation window opens where the related data (the previously modeled tip) is chosen and the tip size in pixel is specified. The tip size in pixel is given by the resolution (in pixel/nm) multiplied by the size of the tip (in nm; which can be e.g. obtained from the vendor's specifications). The resolution of the image can be viewed in *Tools → Statistical quantities*. The noise suppression threshold was set to 100 pm, this value strongly depends on the sample and image quality and can be adjusted according to the noise level.

We recommend to first carry out partial tip estimation and to use the result as input for the full tip estimation run. First, partial tip estimation, which uses only a limited number of the highest points in the image, is applied (*Blind tip estimation → Run partial*), and then full tip estimation (*Blind tip estimation → Run full*), which uses the entire image. This way, the results of the partial tip estimation are used as a starting point for the full estimation and the speed of the full tip estimation is improved. The tip is saved automatically (after clicking *Ok*). Next, the estimated tip shape is used to correct the same or another image (*Data Process → SPM modes → Tip → Surface reconstruction*) – note that the scan pixel size needs to be the same as tip image pixel size (the physical pixel size can be matched manually: *Data Process*

→ *Basic Operations* → *Resample* → *Match pixel size*). Also in Gwyddion, a certainty map can be calculated to view the areas that were not scanned by the apex of the tip but with a side of the tip (*Data Process* → *SPM Modes* → *Tip* → *Certainty Map*). We note, that in our experience the blind tip reconstruction in Gwyddion depends more strongly on the starting values (model tip) than the implementation in SPIP.

Supplementary Table

Parameter	Design	TEM	Dry AFM	Liquid AFM
Width W	10 helices	23 ± 1.2 nm	32.3 ± 1.6 nm (original) 23.3 ± 1.4 nm (reconstr.)	30.0 ± 2.2 nm (original) 28.8 ± 2.9 nm (reconstr.)
Height H1	1 helix	-	0.65 ± 0.3 nm	0.55 ± 0.4 nm
Height H2	2 helices	5.3 ± 0.8 nm	2.1 ± 0.4 nm	2.0 ± 0.5 nm
Height H3	5 helices	12 ± 1 nm	5.4 ± 0.4 nm	9.4 ± 1.4 nm
Height H4	8 helices	19 ± 1.2 nm	8.0 ± 0.4 nm	15.9 ± 1.1 nm
Interhelical spacing (vertical)		2.3 ± 0.1 nm	1.1 ± 0.2 nm	2.0 ± 0.2 nm

Table S1. Dimension analysis of the DNA origami fiducial structure
Comparison of the design dimensions to the dimensions measured in TEM, dry AFM, and liquid AFM. Not all features were consistently visible in the different techniques and are therefore not listed. For the TEM data, the mean and standard deviation are listed. Details about the analysis and the raw data can be found in Supporting Information Figure S1. For the dry and liquid AFM data, Gaussians are fitted to the data (Supporting Information Figure S4) and here the mean and standard deviation of the distribution are listed. We note that the height values are averaged over the full width of the structure.

Supplementary Figures

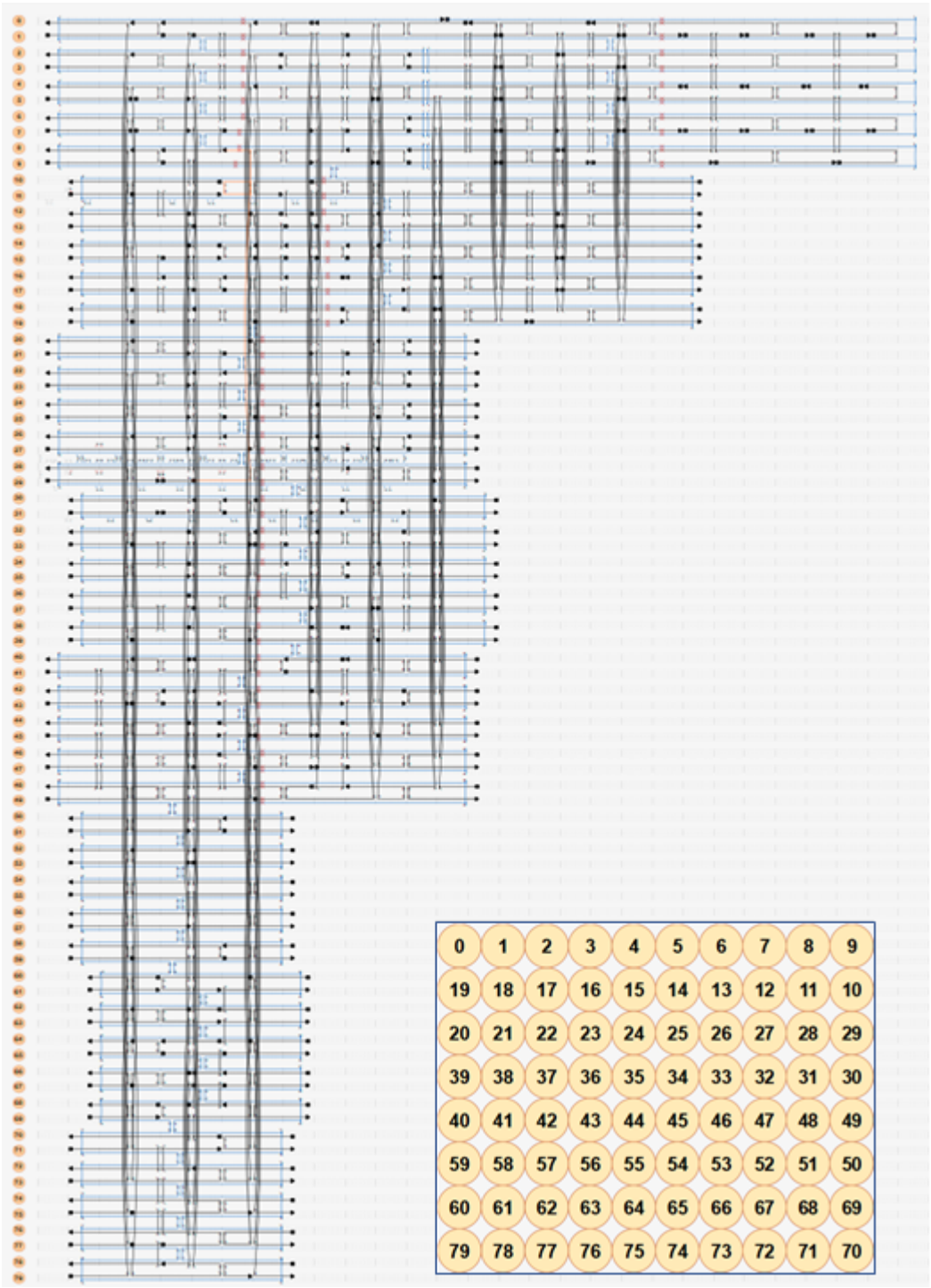

Figure S1. CaDNAno layout of the DNA origami AFM fiducial structure design. The DNA origami AFM fiducial structure was designed using the open-source software caDNAno[1]. The structure consists of four levels, the first two comprising one DNA layer each, the second and fourth three layers each, resulting in a total of eight layers. The DNA helices are arranged in parallel on a square lattice.

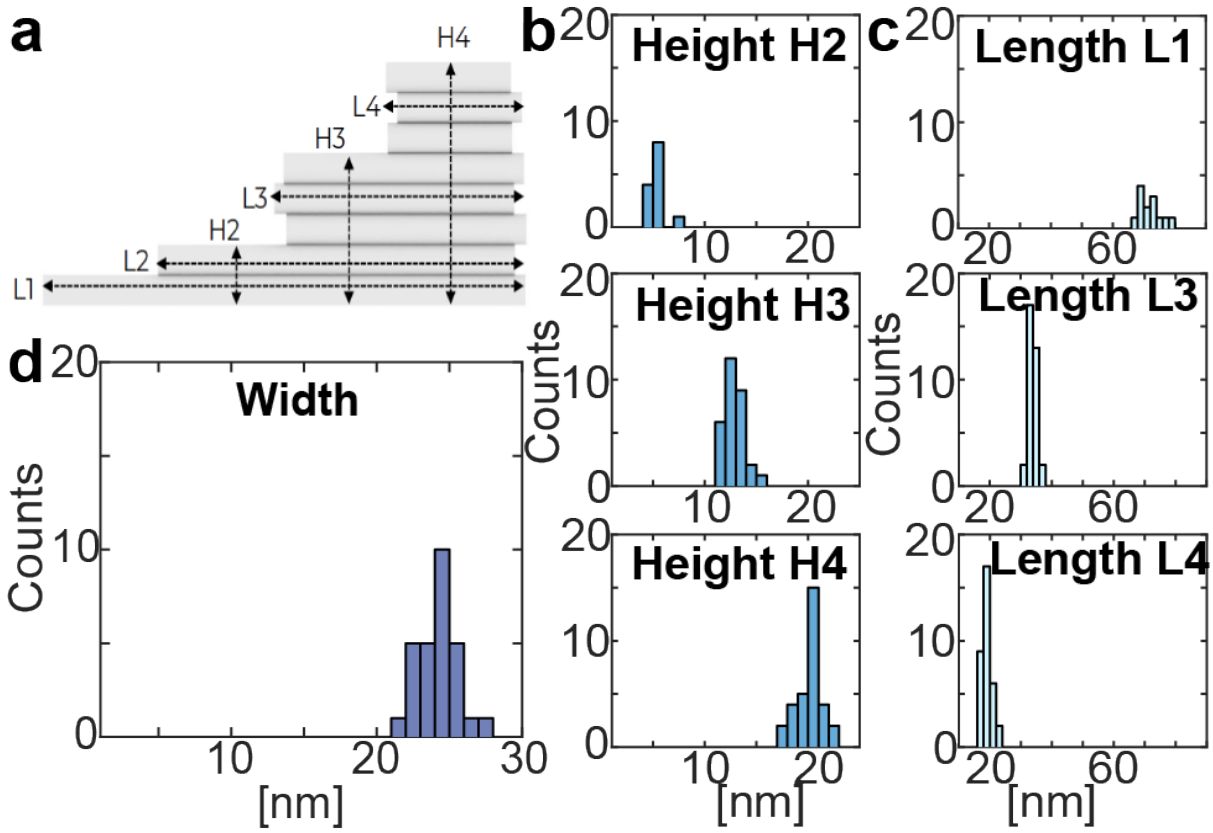

Figure S2. Dimension analysis of the fiducial structures based on TEM images. a) Design of the fiducial structure indicating the design dimensions and labelling of the lengths and heights. b) Height distribution for the 3 highest levels of the fiducial (the lowest level H1 was not visible in the TEM images; see Table S1 for a detailed dimension comparison). c) Length distribution for the levels 1, 3, and 4 of the fiducial (length L2 was not clearly visible in the TEM images). d) Width distribution of the fiducial.

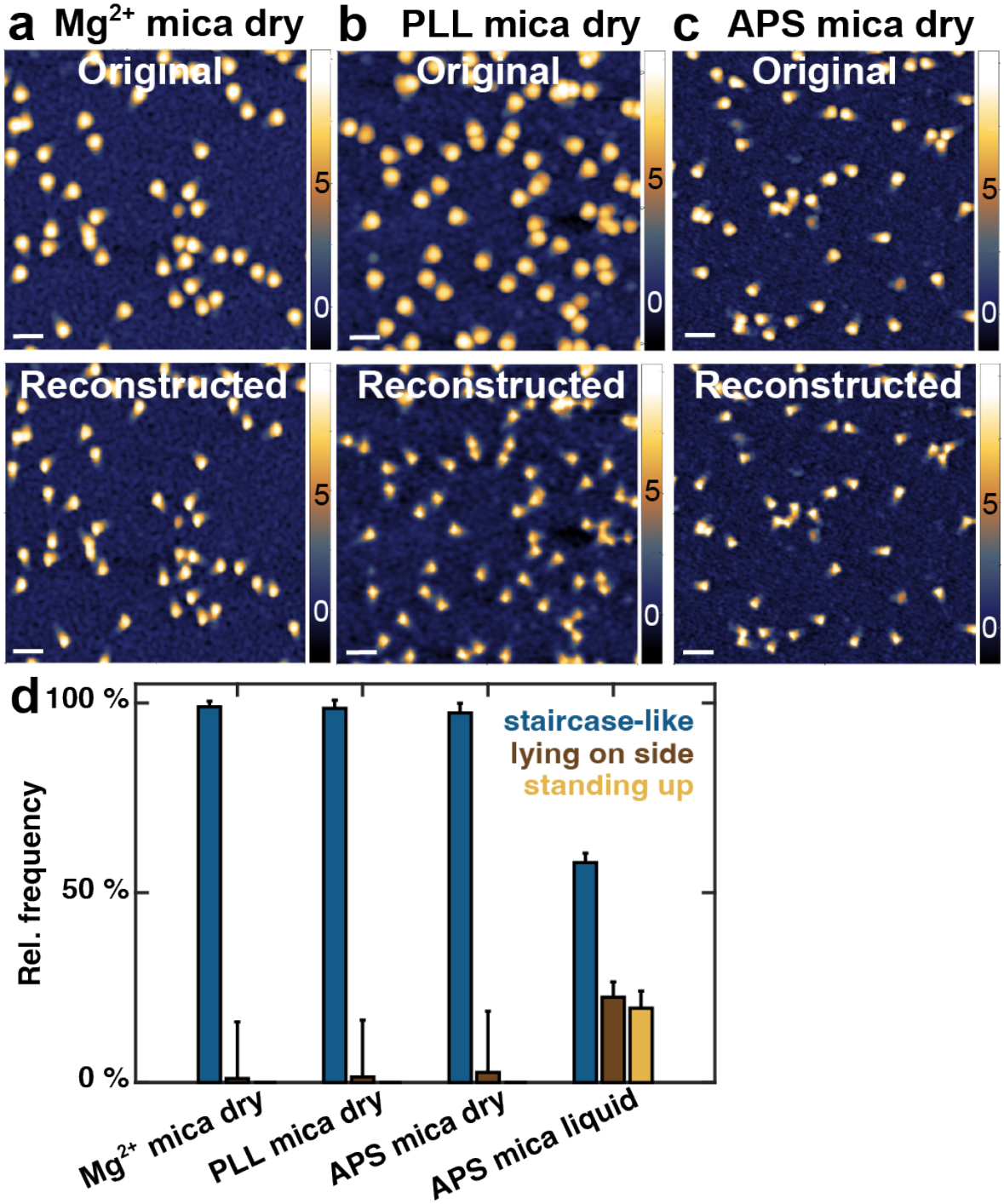

Figure S3. Comparison of AFM images obtained with different surfaces deposition approaches. a) Top: AFM height image of fiducial structures at a concentration of 10 nM deposited on a) Mg^{2+} mica, b) PLL mica, c) APS mica, after drying in air. Bottom: Same images as in top row after reconstruction. The scale bars are 100 nm. Z-ranges are indicated in nm by the scale bars on the right. We note that the variability in image quality visible in the data is mostly due to tip-to-tip variability and not systematically dependent on the deposition method. d) Relative frequency of deposition orientations for Mg^{2+} mica dry, PLL mica dry, APS mica dry, and APS mica liquid. For all tested deposition strategies, the staircase-like orientation is preferred. Only for AFM images acquired in liquid, fiducials lying on their sides or standing upright were also observed in relevant quantities. For all conditions, >300 fiducials from at least three independent measurements were analyzed. The error bars were obtained from counting statistics.

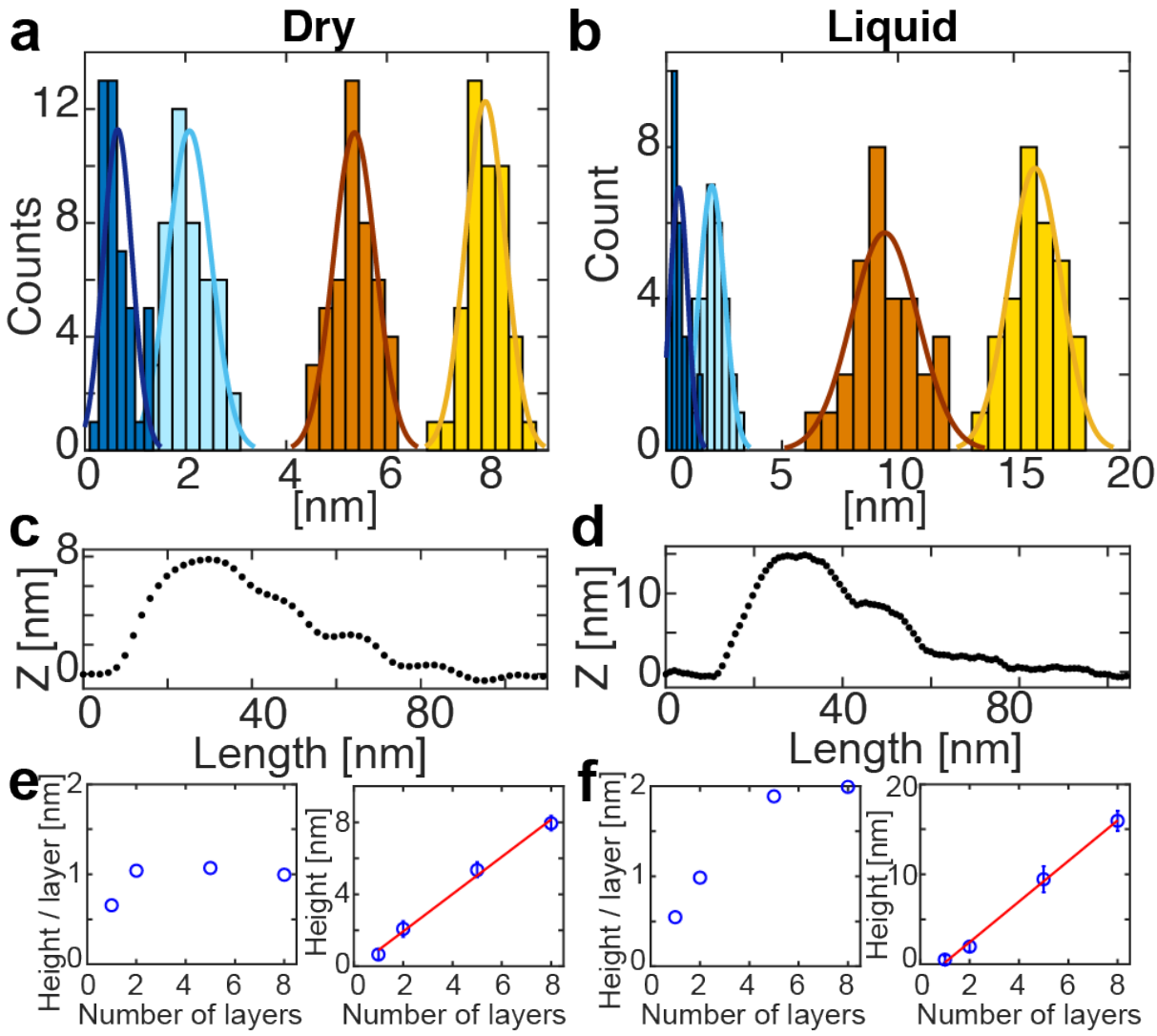

Figure S4. Dimension analysis of the fiducial structures based on AFM images. a) Height distribution for the 4 different levels of the fiducial from dry AFM images and Gaussian fits (solid lines) with Gaussians. b) Height distribution for the 4 different levels of the fiducial from liquid AFM images and Gaussian fits (solid lines). See Table S1 for a detailed dimension comparison. c) One exemplary fiducial height profile from dry AFM imaging. d) One exemplary fiducial height profile from liquid AFM imaging. e) Height per DNA layer and total height as a function of the number of DNA layers in the DNA origami for dry AFM imaging. f) Height per DNA layer and global height as a function of the number of DNA layers in the DNA origami for liquid AFM imaging. The red lines in e and f indicate linear fits. The reported heights are averaged over the full width of the structure. Consequently, the height values represent averages over the helices and the gaps between helices and are, therefore, lower than what the diameter of DNA.

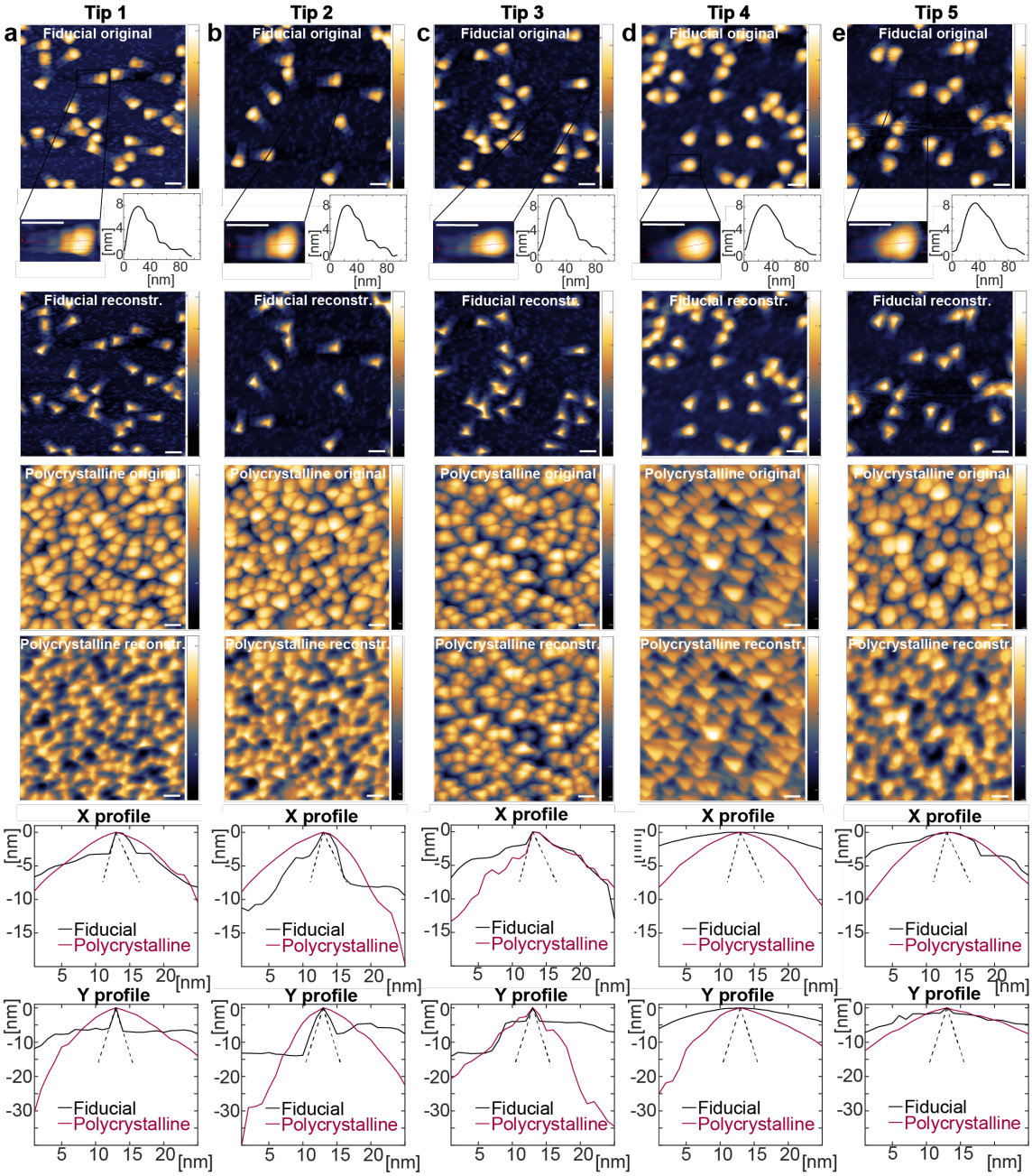

Figure S5. AFM tip characterization using different AFM FASTSCAN-A cantilevers. a) Top: AFM height image of fiducial structures at a concentration of 5 nM on APS mica, measured dry. Total image size is 500 x 500 nm^2 and 512 x 512 pixels. The scale bars are 50 nm. The Z-ranges are indicated in nm by scale bars on the right. One exemplary fiducial structure is shown as a zoom-in as well as its height profile underneath. Third row: Reconstructed image of the AFM image shown in the first row. Fourth row: scan of a polycrystalline sample with the same tip. Total image size is 1 x 1 μm^2 and 1024 x 1024 pixels. Fifth row: Reconstructed image of the AFM image shown in the forth row. The scale bars are 50 nm. The Z-ranges are indicated in nm by scale bars on the right. Sixth and seventh row: AFM tip shape (height profile along x- and y) obtained from blind tip reconstruction using the fiducial sample or the polycrystalline sample, respectively. As a reference, the tip opening angles stated by the vendor are co-plotted as dashed lines. b) – e) Analogous to panel a for different FASTSCAN-A tips from the same batch. The data suggest considerable variation between tips; Tips used for panels a and b enabled high-resolution images and reconstructed tip shapes using our fiducial are close to vendor specifications. Tips used for panels c-e appeared less sharp and gave only lower-resolution images.

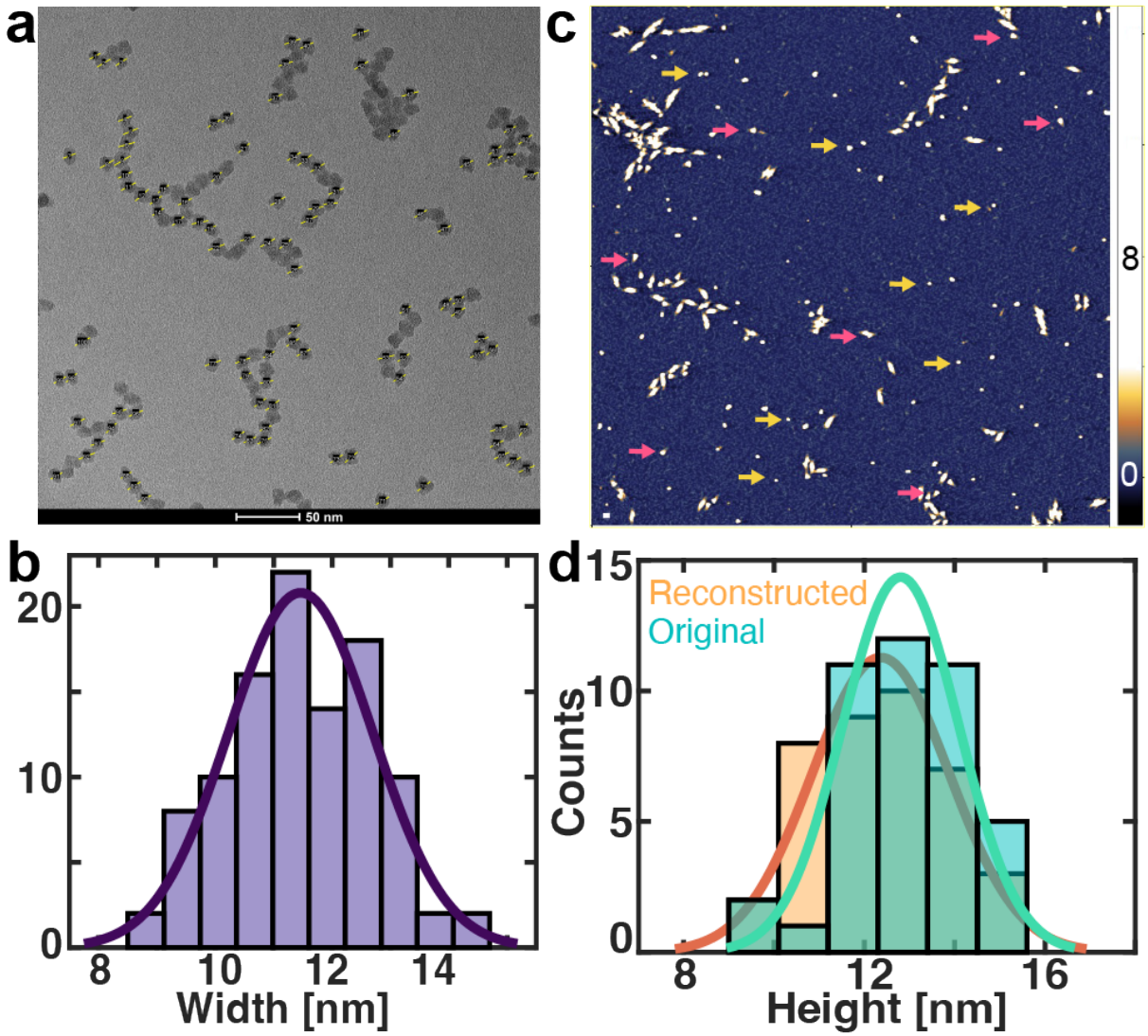

Figure S6. Width analysis of SiO_2 nanoparticles based on TEM images and co-deposition with fiducial structures in AFM with height analysis. a) TEM image of SiO_2 nanoparticles to determine size and shape. Yellow lines indicate cross-sections used for size analysis. b) Width distribution of the SiO_2 nanoparticles from the TEM image shown in panel a with a mean and standard deviation of (11.5 ± 1.2) nm. c) AFM height image of the fiducial structures co-deposited with SiO2 nanoparticles, both at a concentration of 1 nM, deposited on APS mica and measured dry with a resolution of 1 pixel/nm. Exemplary fiducials and nanoparticles are indicated with magenta and yellow arrows, respectively. The scale bar is 50 nm. The Z-range is indicated in nm by the scale bar on the right. d) Height distribution from AFM images before (turquoise) and after (orange) image reconstruction. The solid lines are Gaussian fits. The mean height in the original image of (12.8 ± 1.3) nm (mean ± std) does not change within error after image reconstruction (12.4 ± 1.5) nm by finite tip size correction.

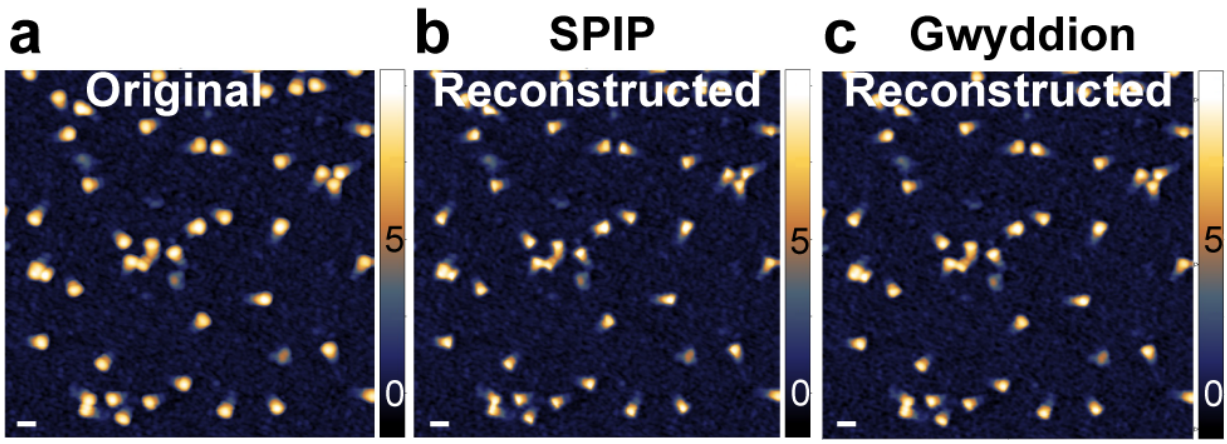

Figure S7. Comparison of AFM image reconstruction softwares. a) AFM height image of fiducial structures at a concentration of 10 nM deposited on APS mica, after drying in air (same image as shown in Supplementary Figure S3c top). b) The image from panel a after reconstruction with the software SPIP (same image as shown in Supplementary Figure S3c bottom). c) The image from panel a after reconstruction with the software Gwyddion. The scale bars are 50 nm. Z-ranges are indicated in nm by the scale bars on the right. The three images shown in this figure are provided as Supplementary Data in the file Image_Reconstruction_Example_SPIP_Gwyddion.zip.

Supplementary References

1. Douglas, S. M.; Marblestone, A. H.; Teerapittayanon, S.; Vazquez, A.; Church, G. M.; Shih, W. M., Rapid prototyping of 3D DNA-origami shapes with caDNAno. *Nucleic Acids Res* **2009,** *37* (15), 5001-6.
2. Korpelainen, V.; Linko, V.; Seppä, J.; Lassila, A.; Kostiainen, M. A., DNA origami structures as calibration standards for nanometrology. *Measurement Science and Technology* **2017,** *28* (3), 034001.
3. Ke, Y.; Douglas, S. M.; Liu, M.; Sharma, J.; Cheng, A.; Leung, A.; Liu, Y.; Shih, W. M.; Yan, H., Multilayer DNA Origami Packed on a Square Lattice. *Journal of the American Chemical Society* **2009,** *131* (43), 15903-15908.
4. Dietz, H.; Douglas, S. M.; Shih, W. M., Folding DNA into Twisted and Curved Nanoscale Shapes. *Science* **2009,** *325* (5941), 725-730.
5. Fischer, S.; Hartl, C.; Frank, K.; Rädler, J. O.; Liedl, T.; Nickel, B., Shape and Interhelical Spacing of DNA Origami Nanostructures Studied by Small-Angle X-ray Scattering. *Nano Letters* **2016,** *16* (7), 4282-4287.
6. Wagenbauer, K. F.; Engelhardt, F. A. S.; Stahl, E.; Hechtl, V. K.; Stömmer, P.; Seebacher, F.; Meregalli, L.; Ketterer, P.; Gerling, T.; Dietz, H., How We Make DNA Origami. *ChemBioChem* **2017,** *18* (19), 1873-1885.
7. Shahabi, S.; Treccani, L.; Rezwan, K., Amino acid-catalyzed seed regrowth synthesis of photostable high fluorescent silica nanoparticles with tunable sizes for intracellular studies. *Journal of Nanoparticle Research* **2015,** *17* (6), 270.
8. de Boer, F. Y.; van Dijk-Moes, R. J. A.; Imhof, A.; Velikov, K. P., Characterization of the Scattering and Absorption of Colored Zein Colloids in Optically Dense Dispersions. *Langmuir* **2019,** *35* (37), 12091-12099.
9. Shlyakhtenko, L. S.; Gall, A. A.; Lyubchenko, Y. L., Mica functionalization for imaging of DNA and protein-DNA complexes with atomic force microscopy. *Methods in molecular biology (Clifton, N.J.)* **2013,** *931*, 295-312.
10. Konrad, S. F.; Vanderlinden, W.; Frederickx, W.; Brouns, T.; Menze, B. H.; De Feyter, S.; Lipfert, J., High-throughput AFM analysis reveals unwrapping pathways of H3 and CENP-A nucleosomes. *Nanoscale* **2021,** *13* (10), 5435-5447.
11. Cherepanov, P.; Surratt, D.; Toelen, J.; Pluymers, W.; Griffith, J.; De Clercq, E.; Debyser, Z., Activity of recombinant HIV-1 integrase on mini-HIV DNA. *Nucleic Acids Res* **1999,** *27* (10), 2202-2210.
12. Villarrubia, J. S., Algorithms for Scanned Probe Microscope Image Simulation, Surface Reconstruction, and Tip Estimation. *J Res Natl Inst Stand Technol* **1997,** *102* (4), 425-454.